

UNIVERSIDADE ESTADUAL DE CAMPINAS
SISTEMA DE BIBLIOTECAS DA UNICAMP
REPOSITÓRIO DA PRODUÇÃO CIENTÍFICA E INTELLECTUAL DA UNICAMP

Versão do arquivo anexado / Version of attached file:

Versão do Editor / Published Version

Mais informações no site da editora / Further information on publisher's website:

<https://www.scielo.br/j/bjmbr/a/VxChNCw46qqXCnpTxKcj6wg>

DOI: 10.1590/S0100-879X2011007500030

Direitos autorais / Publisher's copyright statement:

©2011 by Associação Brasileira de Divulgação Científica. All rights reserved.

DIRETORIA DE TRATAMENTO DA INFORMAÇÃO

Cidade Universitária Zeferino Vaz Barão Geraldo

CEP 13083-970 – Campinas SP

Fone: (19) 3521-6493

<http://www.repositorio.unicamp.br>

Manual and semi-automatic quantification of *in vivo* ^1H -MRS data for the classification of human primary brain tumors

S. Cuellar-Baena^{1,4}, L.M.T.S. Morais^{2,4}, F. Cendes^{3,4}, A.V. Faria^{2,4}
and G. Castellano^{1,4}

¹Departamento de Raios C3smicos e Cronologia, Instituto de F3sica Gleb Wataghin,

²Departamento de Radiologia, ³Departamento de Neurologia, Faculdade de Ci4ncias M3dicas, Universidade de Campinas, Campinas, SP, Brasil

⁴Programa CInAPCe (Coopera33o Interinstitucional de Apoio a Pesquisas sobre o C3rebro), SP, Brasil

Abstract

In vivo proton magnetic resonance spectroscopy (^1H -MRS) is a technique capable of assessing biochemical content and pathways in normal and pathological tissue. In the brain, ^1H -MRS complements the information given by magnetic resonance images. The main goal of the present study was to assess the accuracy of ^1H -MRS for the classification of brain tumors in a pilot study comparing results obtained by manual and semi-automatic quantification of metabolites. *In vivo* single-voxel ^1H -MRS was performed in 24 control subjects and 26 patients with brain neoplasms that included meningiomas, high-grade neuroglial tumors and pilocytic astrocytomas. Seven metabolite groups (lactate, lipids, N-acetyl-aspartate, glutamate and glutamine group, total creatine, total choline, myo-inositol) were evaluated in all spectra by two methods: a manual one consisting of integration of manually defined peak areas, and the advanced method for accurate, robust and efficient spectral fitting (AMARES), a semi-automatic quantification method implemented in the jMRUI software. Statistical methods included discriminant analysis and the leave-one-out cross-validation method. Both manual and semi-automatic analyses detected differences in metabolite content between tumor groups and controls ($P < 0.005$). The classification accuracy obtained with the manual method was 75% for high-grade neuroglial tumors, 55% for meningiomas and 56% for pilocytic astrocytomas, while for the semi-automatic method it was 78, 70, and 98%, respectively. Both methods classified all control subjects correctly. The study demonstrated that ^1H -MRS accurately differentiated normal from tumoral brain tissue and confirmed the superiority of the semi-automatic quantification method.

Key words: Proton magnetic resonance spectroscopy; Brain tumors; AMARES; Tumor classification

Introduction

In vivo proton magnetic resonance spectroscopy (^1H -MRS) is a powerful and promising approach to the measurement of biochemical content and pathways in normal and pathological tissue (1). In the brain, where it is frequently applied, ^1H -MRS complements the information provided by magnetic resonance (MR) images (2,3). Quantification of the main metabolites detected by MRS at long or short echo times can provide quantitative information about these substances, which are involved in different processes in the nervous system. In brain tumors, biochemical pathways such as glycolysis can increase lactate levels, abnormal enzymatic activation can increase total choline (i.e., glycerophosphocholine and phosphocholine) levels, and

neuronal damage can decrease N-acetyl-aspartate (NAA) levels. Also, many other known and unknown pathological conditions related to genetic, osmotic, nutritional, and energetic stresses change the concentrations of these and other detectable metabolites, such as total creatine (i.e., creatine and phosphocreatine) and lipids.

Several studies have been conducted to assess the metabolic patterns of brain tumors in an attempt to correlate them with the histology of the tumor, aggressiveness, and clinical outcome (4-12). Some studies have compared different kinds of spectral fitting methods, either in the time (13) or frequency domain (14). The aim of the present study was to determine the accuracy of the MRS technique for

Correspondence: G. Castellano, Departamento de Raios C3smicos e Cronologia, Instituto de F3sica Gleb Wataghin, UNICAMP, 13083-970 Campinas, SP, Brasil. Fax: +55-19-3521-5512. E-mail: gabriela@ifi.unicamp.br

Received June 18, 2010. Accepted February 11, 2011. Available online March 11, 2011. Published April 11, 2011.

tumor classification. This was achieved by comparing the quantitative data for a control group with that of patients with brain tumors from an MRS database. MRS data quantification was performed using two methods: a manual method and the AMARES (advanced method for accurate, robust and efficient spectral fitting) semi-automatic method (15). An additional objective was to determine whether the semi-automatic method showed any improvement over the manual one. A more accurate measurement of the concentrations of these metabolites can contribute to the improvement of diagnosis and of clinical management, and expand our knowledge about the metabolism of brain tumors.

Material and Methods

Subjects

The ^1H -MRS spectral data used in this study were provided by the Neuroimage Laboratory of the University Hospital, University of Campinas (UNICAMP), Campinas, SP, Brazil. They consisted of spectra acquired from 24 normal subjects (control group) and 26 patients with different types of primary brain tumors. The study was approved by the Ethics Committee of UNICAMP and all subjects gave written informed consent. Subject ages ranged from 14 to 71 years. The control group was not paired by age to the patient group although it is well known that the metabolic pattern of brain tissue is age dependent. In the present study, only tumor tissue was considered and in this case metabolism is much more dependent on the tumor itself. Control subjects ranged in age from 19 to 67 years. Magnetic resonance images were used to place the voxel accurately within the tumor. Also, given the size of the tumors studied, voxel contamination with normal tissue was kept to a minimum.

Patients underwent surgery or a biopsy for the treatment or diagnosis of primary brain tumors. The tissue specimens were processed for routine histopathology. Diagnosis was performed on 10-mm thin cryostat sections after hematoxylin-eosin staining and followed the classification system of the World Health Organization (WHO) (16).

Patients with tumors were divided into three groups according to histological type: group 1: high-grade neu-

roglial (N = 12); group 2: meningiomas (N = 7); group 3: pilocytic astrocytoma (N = 7). Group 4 (control) consisted of 24 subjects. Table 1 provides further information about the patients and tumors. Patients were not receiving any treatment (clinical or surgical), because the scans reported here were the first step in the clinical investigation. Figure 1 shows examples of original and fitted spectra from these groups.

Scanning protocol

MRS data were acquired at 2.0 T using a head coil in an Elscint Prestige Scanner (Haifa, Israel) and a PRESS sequence with repetition time (TR) = 1500 ms, echo time (TE) = 136 ms, 200 repetitions, spectral width (SW) = 1000 Hz, and 1024 complex data points. Voxels were localized in the white matter for the control subjects, whereas for the patients they were positioned inside the tumor volume. All voxels measured $2 \times 2 \times 2 \text{ cm}^3$. Common procedures used in MRS studies, such as automatic shimming, water suppression through CHESS pulses and eddy-currents compensation, were performed for all acquisitions. T_2 -weighted MR images were also acquired in order to visualize the affected area of the brain.

Post-processing and quantification of the signals

The manual post-processing of spectral signals consisted of the use of apodization, varying from 2 to 3 Hz, manual phasing of the spectra, and zero-filling (by a factor of 2). The quantification of metabolites consisted of the integration of peak areas, which was achieved by manually defining the center frequency and the initial and final points of each peak. This procedure was performed directly on the scanner console by a neuroradiologist, and only the main metabolite resonances were quantified: lipids, lactate, NAA, total creatine, choline group, and myo-inositol.

Semi-automatic post-processing of spectral signals was carried out using the jMRUI software (<http://www.mrui.uab.es/mrui/mru-Overview.shtml>). In order to compensate for a small frequency drift of the equipment, the first step taken was to phase the residual water peak in all the spectra acquired for each scan using a reference signal (acquired without water suppression), then to frequency-align these

Table 1. Demographic data of controls and patients with brain tumors.

Group	N	Age (years)	Gender	Diagnosis
High-grade neuroglial tumors	12	53 \pm 13	5 F/7 M	Glioblastomas, anaplastic oligoastrocytomas and anaplastic astrocytomas
Meningiomas	7	59 \pm 7	2 F/5 M	Meningioma
Pilocytic astrocytomas	7	38 \pm 21	3 F/4 M	Pilocytic astrocytoma
Controls	24	33 \pm 14	12 F/12 M	-

Data are reported as means \pm SD. F = female; M = male.

Table 2. Frequency ranges used in the AMARES quantification method.

Metabolite group	Frequency range (ppm)
Lipids	0.85-1.0
Lactate	1.15-1.55
N-acetyl-aspartate	1.98-2.08
Glutamate and glutamine	2.31-2.60
Creatine and phosphocreatine	2.98-3.08
Choline group	3.16-3.26
Myo-inositol	3.36-3.61

Resonance frequency ranges used as prior knowledge in the AMARES method. Ranges were based on values reported in Refs. 6 and 19.

spectra based on the water peak, and averaging these spectra to obtain a higher signal to noise ratio (SNR) spectrum. Next, the residual water signal, centered around 4.68 ppm, was filtered using the Hankel-Lanczos singular value decomposition routine (17). Neither zero filling nor apodization procedures were applied to the data.

The metabolite peaks of interest were quantified using the semi-automatic time-domain quantitation method AMARES (15) implemented in the jMRUI software. To improve the quantification process, this method relies on prior knowledge entered by the user about the sought resonance peaks (18). The frequency ranges shown in Table 2 were used for this purpose. They correspond to the metabolite resonances used as markers in the tumor classification scheme. Ranges were centered on the values reported in Refs. 6 and 19. The abbreviated names of the peaks (resonance ranges) were assigned according to the metabolite with the largest contribution to that peak.

A range for the variation of peak line width was also entered. It was based on prior information. These were allowed to vary between 2-14 Hz. No assumptions were made for metabolite peak amplitudes or phases, with the exception of the relative phase of the lactate peak, which was fixed at 180 degrees, since this resonance inverts at the echo time used (136 ms). Also, Lorentzian line shapes were imposed for spectral fitting.

The AMARES method is a time-domain quantification procedure used to calculate the amplitudes of the metabolites in noisy MR spectra. This method uses the following model function to fit each metabolite peak:

Equation 1

$$y_n = \hat{y}_n + e_n = \sum_{k=1}^K a_k e^{j(\phi_k + 2\pi f_k t_n)} e^{j[-d_k(1-g_k+g_k t_n)]} + e_n, \quad n = 0, 1, \dots, N-1$$

where a_k is the amplitude, ϕ_k is the phase, d_k is the damping factor, and f_k is the frequency of the k -th sinusoid ($k = 1, \dots, K$); $t_n = \Delta t + t_0$ with Δt as the sampling interval, t_0 is the time between the effective time origin and the first data point to be included in the analysis, g_k is a factor that allows choosing between Gaussian ($g_k = 1$) and Lorentzian ($g_k = 0$) line shapes for each peak, and e_n is complex white Gaussian noise. \hat{y} represents the model function, while the actual measurements are represented by y (15).

The AMARES method provided estimates for the peak frequency, amplitude, phase, and line width of the aforementioned resonances (Table 2). In order to compare the quantitation results for different subjects, the peak area of each metabolite was normalized by the sum of all peak areas. Although this sum varied among the individuals considered, we expected this variation to be smaller than the variation of the creatine peak, normally used as internal reference in cerebral ¹H-MRS, since the concentration of this metabolite in tumor varies in unpredictable ways.

Statistical analysis

Linear discriminant analysis (LDA) was used to obtain a classification model for the groups using combinations of metabolite amounts (20,21) and the leave-one-out cross-validation method was applied to assess the reliability of the classifier in our small data set.

Results

Tumor groups

Group 1: High-grade neuroglial tumors. This group, consisting of 12 subjects, contained the most aggressive parenchymal type of tumors: glioblastomas, anaplastic oligoastrocytomas and anaplastic astrocytomas. It was characterized by decreased peak amplitudes of NAA and creatine, metabolic changes usually correlated to neuronal damage and abnormalities in energy metabolism, respectively. The presence of lactate is consistent with tumor aggressiveness. A lipid peak was detected correlating with necrotic tissue, usually present in these tumors (Figure 1A). The manual method correctly classified 75% of the patients for this group, against a 78% correct classification achieved with the AMARES method (see Table 3).

Group 2: Non-neuroglial tumors. This group contained extraparenchymal originating tumors. In the present study, it was composed of 7 meningiomas (tumors that arise from the arachnoidal cap cells of the meninges). The main characteristic of these spectra was the prominent choline signal (Figure 1B). Peaks that characterize brain tissue, such as NAA and creatine, were decreased. The manual method

correctly classified 55% of the subjects and the AMARES method correctly classified 70% of them (see Table 3).

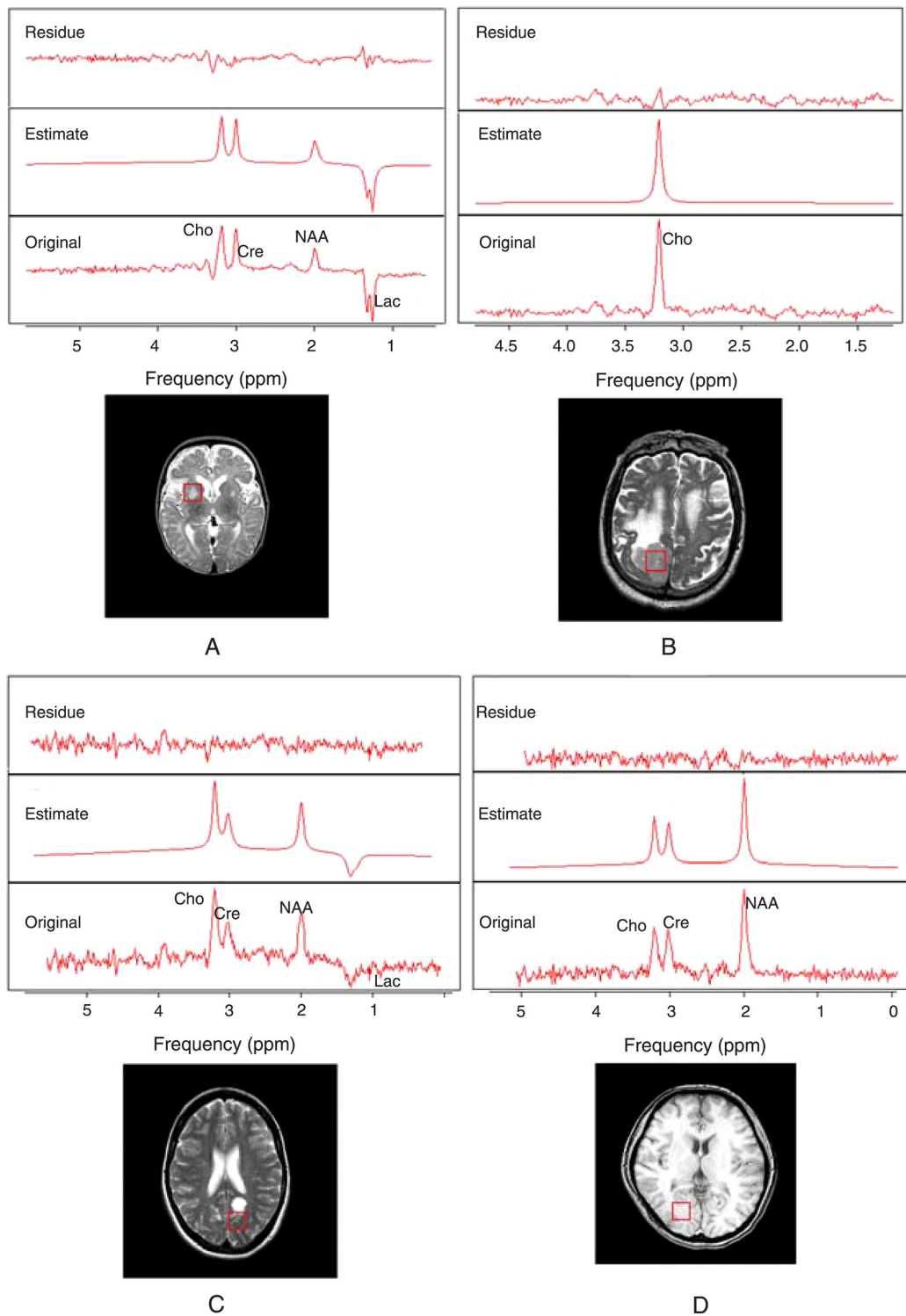


Figure 1. Typical spectra from the tumor and control groups. Typical ^1H -MRS and MRI of patients with A, high-grade neuroglial tumors (group 1); B, meningioma (non-neuroglial tumors, group 2); C, pilocytic astrocytoma (group 3), and D, of a control subject (group 4). ^1H -MRS = proton magnetic resonance spectroscopy; MRI = magnetic resonance imaging; Cho = choline group; Cre = creatine and phosphocreatine; Lac = lactate; NAA = N-acetyl-aspartate.

Group 3: Pilocytic astrocytoma. Pilocytic astrocytoma is a benign neuroglial tumor type, and in this study the corresponding group consisted of 7 subjects. Similar to the high-grade neuroglial group, the spectra of this group were characterized by a decreased NAA and creatine signal and by the presence of lactate (Figure 1C). For this group, the manual method achieved a classification accuracy of 56%, and the AMARES method achieved an accuracy of 98% (see Table 3).

Group 4: Control group. This group was primarily characterized by prominent signals of NAA, choline and creatine, and by the absence of metabolites such as lactate or lipids (see Figure 1D). The control group was correctly identified by both methods in 100% of the cases (see Table 3).

Group classification

Figures 2 and 3 show graphs of the mean values of relative concentrations versus tumor group (groups 1, 2, 3, where 4 is the control group) for each metabolite group (or frequency range) considered. These results are also summarized in Table 3. It can be seen that both the manual and semi-automatic analyses showed differences in mean metabolite amounts between tumor groups and controls ($P < 0.005$). The manual analysis showed a greater standard deviation for the measurement of choline, creatine and myo-inositol peaks. Also, with this method it was not possible to quantify the glutamate/glutamine group: this is one of the limitations of the manual method since, due to the post-

processing techniques used such as apodization, peaks are enlarged and fewer resonances remain detectable.

Table 4 shows the results of LDA (22). As expected, the semi-automatic method achieved a higher classification rate for all tumor groups. Also, differentiation between normal and tumoral tissue was confirmed with both methods.

Figure 4 shows the discriminant distributions of tumor groups for both methods. The factors 1 and 2 in these graphs indicate the main numerical characteristics calculated by LDA that are able to discriminate among groups. These graphs show that the semi-automatic method achieved the best results for tumor groups, showing less variability within groups and better separation between groups. In particular, group 3 (pilocytic astrocytomas) was well separated from the other tumor types by this method. The manual method presented broader and more overlapping distributions.

Discussion

Several factors can interfere with the classification of brain tumors using 136 ms TE metabolite markers from *in vivo* ¹H-MRS signals. Inherent to the technique are: the low SNR resulting from the low-medium magnitude (1-3 Tesla) of the magnetic fields used in clinical applications, together with the low sensitivity of the technique (due to low concentrations of the metabolites studied in the human body); magnetic field inhomogeneities arising from a number of

Table 3. Mean quantification results obtained with the manual and semi-automatic methods.

Metabolites	1 - High-grade neuroglial tumors (N = 12)	2 - Non-neuroglial tumors (N = 7)	3 - Pilocytic astrocytoma (N = 7)	4 - Control (N = 24)
Manual method				
Lipids	0.133 ± 0.262	0	0	0
Lactate	0.079 ± 0.109	0.056 ± 0.072	0.150 ± 0.185	0
NAA	0.072 ± 0.073	0.101 ± 0.105	0.190 ± 0.111	0.282 ± 0.117
Creatine	0.114 ± 0.070	0.154 ± 0.143	0.114 ± 0.094	0.251 ± 0.173
Choline	0.427 ± 0.192	0.580 ± 0.269	0.401 ± 0.178	0.242 ± 0.107
Myo-inositol	0.175 ± 0.099	0.110 ± 0.113	0.146 ± 0.151	0.225 ± 0.250
AMARES method				
Lipids	0.222 ± 0.313	0.276 ± 0.631	0.177 ± 0.245	0
Lactate	0.358 ± 0.405	0.335 ± 0.612	0.260 ± 0.270	0
NAA	0.175 ± 0.143	0.085 ± 0.118	0.211 ± 0.206	0.412 ± 0.122
Glx	0.098 ± 0.064	0.093 ± 0.089	0.100 ± 0.073	0.062 ± 0.032
Creatine	0.187 ± 0.075	0.106 ± 0.107	0.223 ± 0.111	0.266 ± 0.045
Choline	0.425 ± 0.200	0.539 ± 0.315	0.398 ± 0.168	0.265 ± 0.084
Myo-inositol	0.048 ± 0.080	0.043 ± 0.043	0.038 ± 0.057	0.012 ± 0.014

Metabolite data are reported as fractional concentrations, relative to the sum of the concentrations of all metabolites quantified by the method, as means ± standard deviations and were calculated with the manual and semi-automatic (AMARES) quantification methods for the selected tumor groups. NAA = N-acetyl-aspartate; Glx = glutamate/glutamine group.

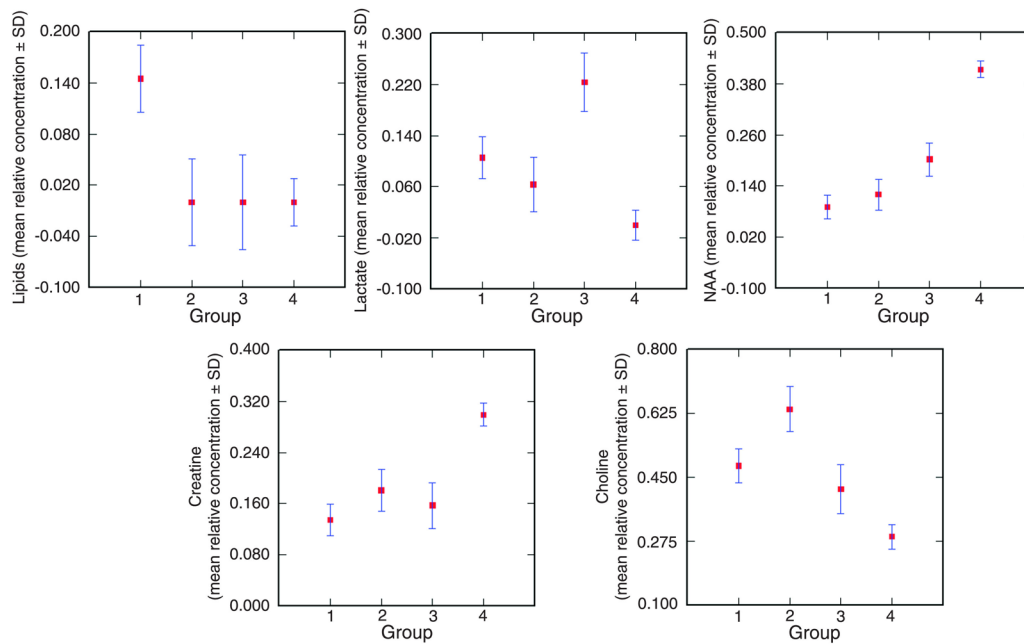


Figure 2. Mean relative concentration \pm SD for each tumor group (1 = high-grade neuroglial, 2 = non-neuroglial, and 3 = pilocytic astrocytoma) and for the control group (4). NAA = N-acetyl-aspartate.

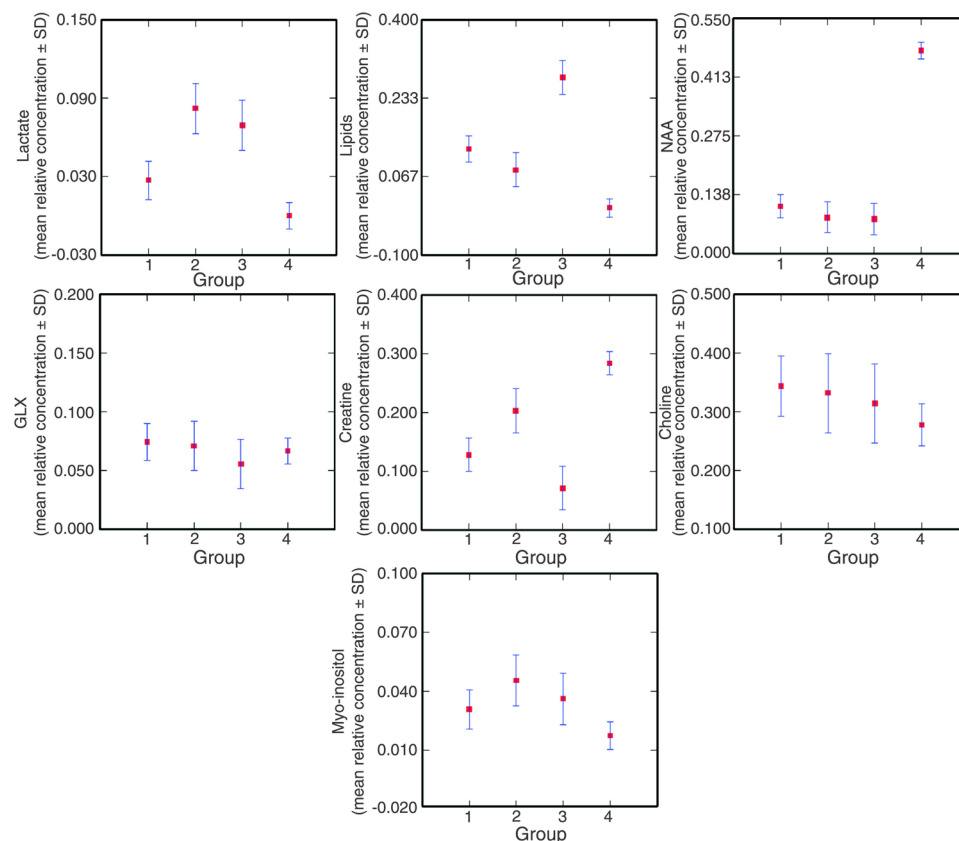


Figure 3. Mean relative concentration \pm SD for each tumor group (1 = high-grade neuroglial, 2 = non-neuroglial, and 3 = pilocytic astrocytoma) and for the control group (4). NAA = N-acetyl-aspartate; Glx = glutamate/glutamine group.

different factors (such as eddy currents) that contribute to the uncertainty of the measurements; the residual signals from water and fat that modify the baseline. Also, long TE spectra compromise the quantification of metabolite groups such as glutamate/glutamine, myo-inositol and lipids due to their shorter T2 constant. These limitations may have influenced our results independently of the quantification method used. Particularly for the manual method, the fact that no filtering of the residual water peak was possible may have compromised the quantification of resonances closest to this peak, for example myo-inositol. Indeed, Table 3 shows a decrease of myo-inositol for tumor groups compared to the control group for the manual method, while it shows an increase of this metabolite for the tumor groups compared to the control group for the semi-automatic method. The myo-inositol decrease with the manual method was probably due to errors in the setting of peak limits. The manual procedure tends to restrict peak limits to what really stands out from the baseline, and since the residual water peak was not filtered in this procedure, the baseline around the myo-inositol peak was probably increased, reducing the peak limits and consequently the measured area.

From Table 4, we see that the results obtained with the manual method for differentiating between normal (control) and tumoral tissue were relatively good (a 92% correct classification as tumor or normal). However, the individual tumor classification accuracy was much lower (75, 55, and 56% for the three tumor groups). This is clearly due to the fact that, as can be seen in Figure 1, normal spectra are quite different from spectra obtained from the types of tumor considered,

making it easier for the classifier to differentiate between these two types of spectra, while spectra from groups 1 (neuroglial tumors) and 3 (pilocytic astrocytomas) are more similar, probably accounting for the lower classification rate. Indeed, we found that the more important metabolites that could be used to differentiate among individual tumor groups were lactate/lipids to differentiate between the three groups with both methods; choline to differentiate between group 2 (non-neuroglial) and the other groups with the manual method, and creatine to differentiate between group 2 and the others with the semi-automatic method.

Also, we agree with Lukas et al. (6) that a limited number of patients in each group makes it difficult to build a classifier with a high generalization capacity. In addition, noise due to artifacts, as mentioned earlier, can reduce the quality of spectral data and consequently impair the calculation of metabolite concentrations, even using a semi-automatic method. This partially explains the fact

Table 4. Classification accuracy for different tumor types, and for normal versus tumoral tissue.

Group	N	Semi-automatic method	Manual method
Controls	24	100%	100%
Tumors	26	92%	92%
1 - Neuroglial	12	78%	75%
2 - Non-neuroglial	7	70%	55%
3 - Pilocytic astrocytoma	7	98%	56%

Data are reported as percent of correct classification obtained by linear discriminant analysis tested by the leave-one-out method to differentiate between normal and tumoral tissue and between tumor types.

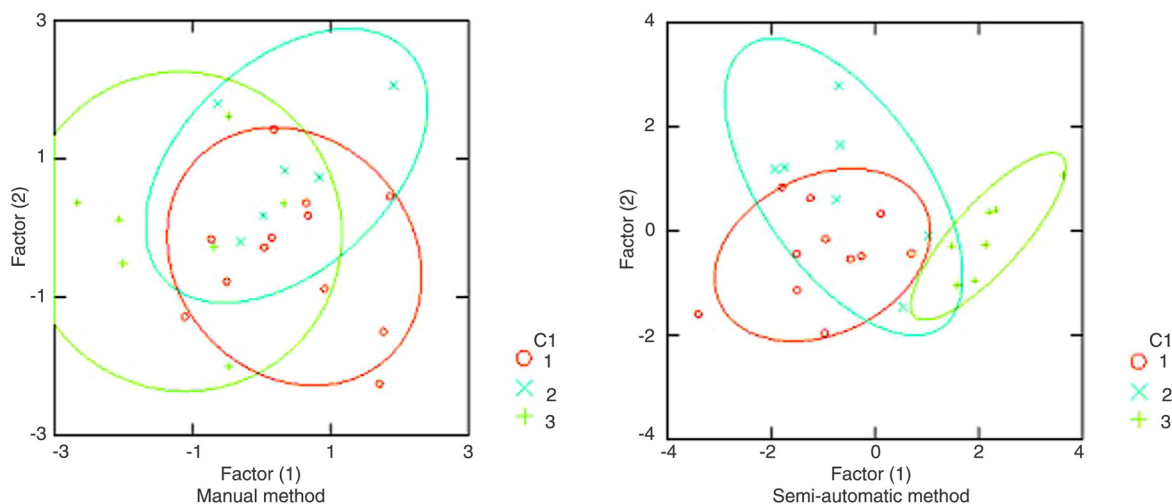


Figure 4. Discriminant distributions of tumor groups for the manual (left) and semi-automatic (right) methods. Red corresponds to high-grade neuroglial tumors (group 1), blue to non-neuroglial tumors (group 2) and green to pilocytic astrocytomas (group 3).

that we have a pronounced overlap between the spectra of different tumor groups.

Even with these limitations, using both manual and semi-automatic analyses, we found a metabolic pattern in tumors and controls that was consistent with recent studies (3,4,6,7,23-27). Tumors showed a reduction in the levels of NAA and creatine and an increase in the levels of choline, compared to normal tissue. Also, some tumor groups showed the presence of lactate and lipid peaks in their spectra, which are not usually seen in healthy tissue. It is important to note that both methods identified all controls correctly, confirming the efficacy of the MRS technique for discriminating between normal and pathological tissue. The most evident difference between the manual and semi-automatic analyses was the more specific classification of high-grade tumors obtained with the latter. We attribute this improvement mainly to consistency of the AMARES method for the measurement of the creatine and choline peaks. Due to the apodization used in the manual procedure, these peaks often semi-overlapped, causing a wide variation in the manual determination of peak limits. This was confirmed by the higher standard deviations of these

measurements and was particularly true in high-grade neuroglial tumors, where the cell heterogeneity and the microscopic areas of necrosis can cause a global decrease in peak amplitude and damage resolution. Also, in general, the manual method involves more sources of error than the semi-automatic one, mainly due to dependency on analyst subjectivity, particularly in the phasing procedure.

We confirmed that manual and semi-automatic analyses of MR spectra are able to differentiate normal from tumoral tissue. The semi-automatic analysis was more accurate in classifying all tumor groups. The semi-automatic method was acceptable to build a model for classifying the tumor types studied here by their histological diagnosis and, despite the small number of subjects included in the study, the manual and semi-automatic methods were in agreement. We believe that a better classification of brain tumors according to clinical parameters will be possible by expanding our sample database.

Acknowledgments

Research supported by FAPESP and CNPq.

References

1. Preul MC, Caramanos Z, Collins DL, Villemure JG, Leblanc R, Olivier A, et al. Accurate, noninvasive diagnosis of human brain tumors by using proton magnetic resonance spectroscopy. *Nat Med* 1996; 2: 323-325.
2. Del Sole A, Falini A, Ravasi L, Ottobriani L, De Marchis D, Bombardieri E, et al. Anatomical and biochemical investigation of primary brain tumours. *Eur J Nucl Med* 2001; 28: 1851-1872.
3. Nakaiso M, Uno M, Harada M, Kageji T, Takimoto O, Nagahiro S. Brain abscess and glioblastoma identified by combined proton magnetic resonance spectroscopy and diffusion-weighted magnetic resonance imaging - two case reports. *Neurol Med Chir* 2002; 42: 346-348.
4. Lehnhardt FG, Bock C, Rohn G, Ernestus RI, Hoehn M. Metabolic differences between primary and recurrent human brain tumors: a ^1H NMR spectroscopic investigation. *NMR Biomed* 2005; 18: 371-382.
5. Demaerel P, Johannik K, Van Hecke P, Van Ongeval C, Verellen S, Marchal G, et al. Localized ^1H NMR spectroscopy in fifty cases of newly diagnosed intracranial tumors. *J Comput Assist Tomogr* 1991; 15: 67-76.
6. Lukas L, Devos A, Suykens JA, Vanhamme L, Howe FA, Majos C, et al. Brain tumor classification based on long echo proton MRS signals. *Artif Intell Med* 2004; 31: 73-89.
7. Tate AR, Majos C, Moreno A, Howe FA, Griffiths JR, Arus C. Automated classification of short echo time in *in vivo* ^1H brain tumor spectra: a multicenter study. *Magn Reson Med* 2003; 49: 29-36.
8. Majos C, Julia-Sape M, Alonso J, Serrallonga M, Aguilera C, Acebes JJ, et al. Brain tumor classification by proton MR spectroscopy: comparison of diagnostic accuracy at short and long TE. *AJNR Am J Neuroradiol* 2004; 25: 1696-1704.
9. Simonetti AW, Melssen WJ, Szabo de Edelenyi F, van Asten JJ, Heerschap A, Buydens LM. Combination of feature-reduced MR spectroscopic and MR imaging data for improved brain tumor classification. *NMR Biomed* 2005; 18: 34-43.
10. Sjobakk TE, Johansen R, Bathen TF, Sonnewald U, Kvistad KA, Lundgren S, et al. Metabolic profiling of human brain metastases using *in vivo* proton MR spectroscopy at 3T. *BMC Cancer* 2007; 7: 141.
11. Garcia-Gomez JM, Luts J, Julia-Sape M, Krooshof P, Tortajada S, Robledo JV, et al. Multiproject-multicenter evaluation of automatic brain tumor classification by magnetic resonance spectroscopy. *MAGMA* 2009; 22: 5-18.
12. Alusta P, Im I, Pearce BA, Beger RD, Kretzer RM, Buzatu DA, et al. Improving proton MR spectroscopy of brain tissue for noninvasive diagnostics. *J Magn Reson Imaging* 2010; 32: 818-829.
13. Vanhamme L, Sundin T, Hecke PV, Huffel SV. MR spectroscopy quantitation: a review of time-domain methods. *NMR Biomed* 2001; 14: 233-246.
14. Mierisova S, Ala-Korpela M. MR spectroscopy quantitation: a review of frequency domain methods. *NMR Biomed* 2001; 14: 247-259.
15. Vanhamme L, van den Boogaart A, Van Huffel S. Improved method for accurate and efficient quantification of MRS data with use of prior knowledge. *J Magn Reson* 1997; 129: 35-43.
16. Louis DN, Ohgaki H, Wiestler OD, Cavenee WK, Burger PC, Jouvet A, et al. The 2007 WHO classification of tumours of the central nervous system. *Acta Neuropathol* 2007; 114: 97-109.
17. Laudadio T, Mastronardi N, Vanhamme L, Van Hecke P, Van

- Huffel S. Improved Lanczos algorithms for blackbox MRS data quantitation. *J Magn Reson* 2002; 157: 292-297.
18. de Graaf AA, Bovee WM. Improved quantification of *in vivo* ¹H NMR spectra by optimization of signal acquisition and processing and by incorporation of prior knowledge into the spectral fitting. *Magn Reson Med* 1990; 15: 305-319.
 19. Govindaraju V, Young K, Maudsley AA. Proton NMR chemical shifts and coupling constants for brain metabolites. *NMR Biomed* 2000; 13: 129-153.
 20. Altman DG. *Practical statistics for medical research*. London: Chapman and Hall; 1991.
 21. Campbell MJ, Machin D. *Medical statistics: a commonsense approach*. Chichester: John Wiley; 1999.
 22. McLachlan GJ. *Discriminant analysis and statistical pattern recognition*. New York: John Wiley; 1992.
 23. Opstad KS, Ladroue C, Bell BA, Griffiths JR, Howe FA. Linear discriminant analysis of brain tumour (1)H MR spectra: a comparison of classification using whole spectra versus metabolite quantification. *NMR Biomed* 2007; 20: 763-770.
 24. Morales H, Kwock L, Castillo M. Magnetic resonance imaging and spectroscopy of pilomyxoid astrocytomas: case reports and comparison with pilocytic astrocytomas. *J Comput Assist Tomogr* 2007; 31: 682-687.
 25. Di Costanzo A, Scarabino T, Trojsi F, Giannatempo GM, Popolizio T, Catapano D, et al. Multiparametric 3T MR approach to the assessment of cerebral gliomas: tumor extent and malignancy. *Neuroradiology* 2006; 48: 622-631.
 26. Cho YD, Choi GH, Lee SP, Kim JK. ¹H-MRS metabolic patterns for distinguishing between meningiomas and other brain tumors. *Magn Reson Imaging* 2003; 21: 663-672.
 27. Howe FA, Barton SJ, Cudlip SA, Stubbs M, Saunders DE, Murphy M, et al. Metabolic profiles of human brain tumors using quantitative *in vivo* ¹H magnetic resonance spectroscopy. *Magn Reson Med* 2003; 49: 223-232.